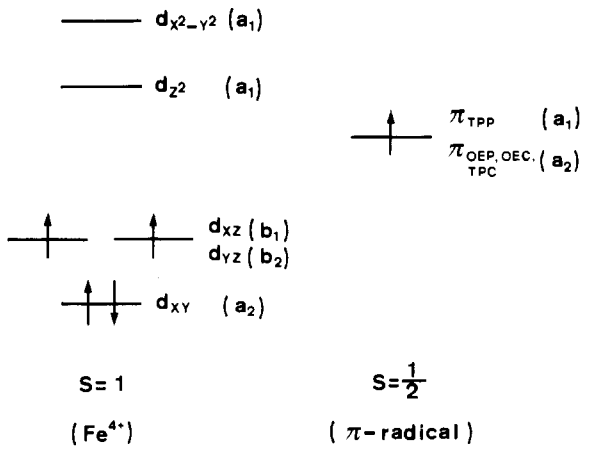

Figure 7. Symmetries of d orbitals and π orbitals under C_{2v} symmetry.

II. The A_1 radical orbital of TPP has the same symmetry as $d_{x^2-y^2}$ and d_{z^2}. Under such lower symmetry the overlap of the radical orbital with two metal orbitals becomes symmetrically allowed. This causes antiferromagnetic coupling, giving a resultant S = 2 ground state. The same description can be used for the OEP and OEC systems. However, the radical orbital of A_2 symmetry in these systems has a smaller amount of spin density on the nitrogens as compared with the case of TPP, so that the magnitude of the coupling becomes smaller than that of the TPP system. Thus it is consistent with the experimental results that antiferromagnetic coupling of OEP (-20 cm^{-1}), OEC (-8 cm^{-1}), and TPC (-85 cm^{-1}) is smaller than that of TPP (-200 cm^{-1}).

Application to the Symmetry of HRP Compound I and MPO Compound I. We now discuss the symmetries of the radical orbitals of HRP compound I and MPO compound I. The magnetic properties of the six-coordinate OEP and OEC systems described above resemble those of HRP compound I or MPO compound I. It is suggested that the iron(IV) S = 1 spin weakly couples with the π radical antiferromagnetically.

Assuming C_{2v} symmetry in these native enzymes, each d orbital has the symmetry shown in Figure 7. From our results and those for the TPP system, two possibilities can be deduced depending on whether the π radical has A_2 symmetry like the OEP and OEC systems or A_1 symmetry like the TPP system. If the π radical of the enzyme has A_1 symmetry, it does not have the same symmetry as the electron-occupied d orbitals, because the d orbitals with the same symmetry, such as $d_{x^2-y^2}$ and d_{z^2}, are empty. Since all the orbitals are orthogonal, the coupling should be ferromagnetic from the results of the TPP system. On the other hand, if the π radical has A_2 symmetry, it has the same symmetry as the d_{xy} orbital. However, it is fully occupied and other half-occupied orbitals are also orthogonal to each other. Then it is deduced from the results for the six-coordinate complexes of the OEP and OEC systems that the coupling should be weakly antiferromagnetic. Experimental results of the native enzymes suggesting weak antiferromagnetic coupling support our proposal that they have orbitals of A_2 or A_{1u} symmetry.

Conclusion

In the OEP and OEC systems the Fe(III) ($S = {}^5/_2$) and the π radical ($s = {}^1/_2$) couple antiferromagnetically in the five-coordinate complexes and weakly couple antiferromagnetically in the six-coordinate ones. This is caused by the symmetry of the π radical, which is A_{1u} in these systems. And from the results for the model complexes, the symmetries of the radical orbitals of HRP compound I and MPO compound I are suggested to be A_{1u} rather than A_{2u}.

Acknowledgment. This work was partially supported by a Grant-in-Aid for Scientific Research on the Priority Area of "Macromolecular Complexes" (No. 63612005), from the Ministry of Education, Science, and Culture, Japan.

Registry No. **1**, 130063-78-4; **2**, 100333-81-1; **3**, 130063-79-5; **4**, 130063-81-9; **5**, 130063-83-1; HRP compound I, 62628-26-6; MPO compound I, 9003-99-0.

Contribution from the Departments of Chemistry, Georgetown University, Washington, D.C. 20057, and Northeastern University, Boston, Massachusetts 02115

Unusually Strong Antiferromagnetic Coupling in Unsymmetrical Diiron(III) μ-Oxo Complexes

Pedro Gomez-Romero,*[1a,b] E. H. Witten,[1c] William Michael Reiff,[1c] and Geoffrey B. Jameson*[1a]

Received November 14, 1989

The complex $[N6FeOFeCl_3]Cl{\cdot}0.5HCl{\cdot}3H_2O{\cdot}2C_2H_5OH$, where N6 is the potentially hexadentate ligand *N,N,N',N'*-tetrakis((2-benzimidazolyl)methyl)ethanediamine, shows distinctively strong antiferromagnetic coupling ($J = -126$ (1) cm^{-1}), more typical of multiply bridged diiron(III) μ-oxo species than of singly bridged species. The X-ray crystal and molecular structure shows a single oxo bridge linking an octahedrally coordinated Fe(III)—one benzimidazole group of ligand N6 does not coordinate—with a tetrahedrally coordinated Fe(III). Some key metrical details are as follows: O-$FeCl_3$, 1.745 (7) Å; O-FeN6, 1.791 (7) Å; Fe-O-Fe, 153.2(4)°; average Fe-Cl 2.20 (1) Å; average Fe-N_{Im}, 2.08 (2) average Fe-N_{amine}, 2.32 (4) Å. Infrared spectroscopy reveals a strong doublet at 833 and 850 cm^{-1} that is associated with the Fe-O-Fe moiety; the latter band is assigned to ν_{as}(Fe-O-Fe). An analysis of orbital interactions reveals how low symmetry (at most, idealized C_s) can facilitate stronger antiferromagnetic coupling than occurs for more symmetrical (C_{2v}) singly bridged diiron(III) μ-oxo species. The distinctive magnetic and vibrational properties associated with these unsymmetrical species extends the range of spectroscopic behavior associated with diiron(III) μ-oxo species, with important consequences in the application of these techniques to dinuclear iron proteins. Relevant crystal and refinement data include the following: monoclinic space group $P2_1/n$; a = 13.775 (4), b = 26.911 (7), c = 13.758 (4) Å; β = 96.24 (2)°; d_{obs} = 1.28 (2), d_{calc} = 1.29 g cm^{-3} for Z = 4; 4231 retained data with $I > 0$ in the range $0.10 < \lambda^{-1} \sin\theta < 0.5399$ $Å^{-1}$; graphite-monochromated Mo Kα radiation (λ = 0.7107 Å); $R(F^2$, all data) = 0.19, $R_w(F^2)$ = 0.22; for the 2126 data for which $I > 3\sigma(I)$, $R(F)$ = 0.088 and $R_w(F)$ = 0.104.

Many symmetrical diiron(III) μ-oxo complexes are known.[2,3] In biological occurrences of this moiety the two iron atoms are often spectroscopically distinct in Mössbauer spectroscopy and unsymmetrical species are inferred.[3] Thus the spectroscopic, magnetic, and structural consequences of asymmetry and of

* To whom correspondence should be addressed.

(1) (a) Georgetown University. (b) Institut de Ciencia de Materiales de Barcelona, Marti i Franques s/n, 08028 Barcelona, Spain. (c) Northeastern University.

0020-1669/90/1329-5211$02.50/0

different ligand combinations in simple complexes are of fundamental importance in developing reliable spectroscopic methodology for the identification of the Fe^{III}–O–Fe^{III} motif in biological systems, especially since the protein matrix may provide unusual ligands and stabilize unusual geometries. While the compound to be reported in this paper does not purport to be a particular model for any currently known metalloprotein, the profound asymmetry of $[N6FeOFeCl_3]^+$, where N6 is the potentially

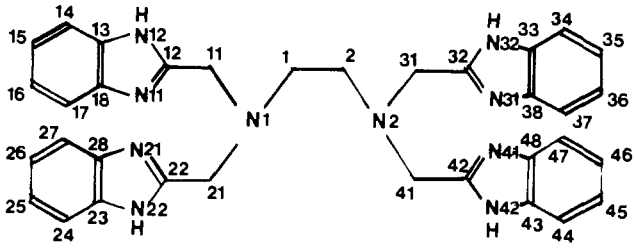

ligand N6, showing atom numbering

hexadentate ligand, *N,N,N',N'*-tetrakis((2-benzimidazolyl)-methyl)-1,2-ethanediamine, has remarkable effects on spectroscopic and magnetic properties. Stronger than usual antiferromagnetic coupling and distinctive vibrational features are observed,[4] thereby extending the range of spectroscopic behavior associated with the Fe^{III}–O–Fe^{III} motif. This paper amplifies the results reported earlier for the complex $[N5FeOFeCl_3]^+$, where N5 is identical with ligand N6 except that one benzimidazole has been replaced by a 2-hydroxyethyl group,[4,5] by offering a simple theoretical basis for the effects of asymmetry.

Experimental Methods

Synthesis of *N,N,N',N'*-Tetrakis((2-benzimidazolyl)methyl)-1,2-ethanediamine (N6). This was prepared by a modification of the method previously reported.[6] Thus, 9.745 g of EDTA (*N,N,N',N'*-ethylenediaminetetraacetic acid) (0.033 mol) and 21.69 g of *o*-phenylenediamine (0.2 mol) were ground and thoroughly mixed together, followed by heating of the mixture in a paraffin oil bath at 180–190 °C, with stirring. After 60 min, when effervescence had ceased, the mixture was cooled and 150 mL of 4 M HCl was added to the glass. The bluish precipitate obtained after several hours was filtered out, washed by slurrying in acetone, and dried in air to give the HCl salt of N6. The salt was dissolved in water with heating and neutralized by addition of a 1:9 concentrated ammonia–water mixture. The wet precipitate obtained by filtration was recrystallized from acetone to give an off-white solid in 47% yield. Anal. Found (calcd) for $C_{34}H_{32}N_{10}\cdot C_3H_6O$ (acetone): C, 71.41 (69.57); H, 6.42 (6.00); N, 18.60 (21.93). This solid was spectroscopically identical with that reported previously.[6a]

Preparation of $[N6FeOFeCl_3]Cl\cdot 3H_2O\cdot 2CH_3OH\cdot 0.5HCl$. This was prepared similarly to its N5 analogue.[4,5] Accordingly, 0.232 g of $FeCl_3\cdot 6H_2O$ (0.86 mmol) was added to a solution of 0.208 g of N6 (0.33 mmol) in 10 mL of absolute ethanol, giving a dark red solution. The crystalline material obtained by evaporation was filtered out, washed with ethanol, and dried at 105 °C in an oven to give 0.27 g of the complex. This was dissolved in 30 mL of boiling methanol, and the mixture filtered; after 2 days of slow evaporation, 0.163 g of red brown crystals was isolated from the mother liquor and dried in air (48% yield). Anal. Found (calcd) for $C_{34}H_{32}N_{10}OFe_2Cl_4\cdot 3H_2O\cdot 2CH_3OH\cdot 0.5HCl$ (fw = 986.57): C, 44.04 (43.85); H, 4.49 (4.70); N, 14.66 (14.20); Cl, 17.29 (16.18); Fe, 11.52 (11.33). This preparation provided the material for the magnetic susceptibility study. For the X-ray diffraction study, crystals from a parallel preparation were sealed with mother liquor in thin-walled glass capillaries to prevent loss of the solvate species.

Table I. Crystallographic Data for $[N_6FeOFeCl_3]Cl\cdot 0.5HCl\cdot 3H_2O\cdot 2CH_3OH$

$Fe_2Cl_{4.5}C_{36}H_{46.5}N_{10}O_6$	fw 986.57
a = 13.775 (4) Å	D_o [D_c] = 1.28 (2) [1.29] g cm^{-3}
b = 26.911 (7) Å	T = 298 K
c = 13.758 (4) Å	λ = 0.7107 Å (graphite monochr)
$\alpha = \gamma = 90°$	μ = 8.25 cm^{-1}
β = 96.24 (2)°	rel transm coeff = 0.91–0.99[a]
V = 5070 (4) Å^3	no. of data with $I > 3\sigma(I)$ = 2126
Z = 4	0.100 < λ^{-1} sin θ < 0.540 Å^{-1}
$P2_1/n$	$R(F)$ [$R_w(F)$] = 0.088 [0.104]

[a] Calculated; no correction made; see Experimental Methods.

X-ray Crystallographic Study of $[N6FeOFeCl_3]Cl\cdot 3H_2O\cdot 2CH_3OH\cdot 0.5HCl$. Monoclinic symmetry and systematic absences uniquely consistent with the space group $P2_1/n$ were observed by precession photography. Crystal orientation and precise unit cell dimensions were determined by least-squares refinement of the setting angles of 20 reflections in the range 0.293 < λ^{-1} sin θ < 0.317 Å^{-1} for a needle-shaped crystal (0.60 × 0.25 × 0.25 mm) mounted with the needle axis approximately coincident with the diffractometer ϕ axis. A Picker FACS-I diffractometer with NRC-Canada software (E. Gabe) was used for this and data collection, during which three standard reflections were monitored every 100 reflections. Although no significant variations were detected in their intensities, the data from a substantial number of other reflections were incorrectly passed to the computer because of an intermittent problem in the power supply to the computer interface. Where identifiable, these reflections, characterized by anomalously high values of intensity, have been deleted. A total of 406 reflections (out of a total of 4637 scanned for the quadrant $\pm h,+k,+l$) were deleted at a late stage in refinement, after all non-hydrogen atoms were located and included in the model. While we are left with less than optimal data and precision in derived parameters, the accuracy of the structure of the cation has not been compromised, as evidenced by the fact that chemically equivalent bonds in the benzimidazole moiety have statistically insignificant differences—this was not so before deletion of defective data—and physically reasonable atom displacement parameters for the atoms of the coordination sphere that were refined anisotropically. Data collection and final refinement parameters and crystal data are summarized in Table I. A fuller tabulation is available as Table S-I (supplementary material). The structure was solved by direct methods (MULTAN82) and developed by difference Fourier maps and least-squares refinement, as incorporated in the SDP V3.0 (Enraf Nonius). In addition to the well-defined cation, a chloride counterion, two methanol and three water molecules of solvation, and a half-molecule of (H)Cl were unambiguously located. Hydrogen atoms were included as a fixed contribution to F_c but were not refined. Final refinements were upon F^2, with all 4231 retained data, leading to $R(F^2)$ and $R_w(F^2)$ of 0.194 and 0.217, respectively. The minimized function was independent of h,k,l and combinations thereof and of diffraction geometry and only weakly dependent upon ranges of λ^{-1} sin θ and the magnitude of F_o (weighting scheme: $1/w = \sigma^2$(counting) + $(0.07F^2)^2$). The final difference map was featureless. Final atomic parameters and isotropic displacement factors of refined atoms are given in Table II. Tabulations of all positional and isotropic thermal parameters and anisotropic thermal parameters (Tables S-II and S-III), bond distances and angles (Tables S-IV and S-V), and selected torsion angles (Table S-VI) are available as supplementary material.

Magnetic Susceptibility. Magnetic susceptibility data were recorded at the University of Virginia on a Biomagnetic Technology (formerly SHE Corp.) SQUID susceptometer in the range 7–300 K. Molar susceptibilities were corrected for intrinsic diamagnetism corresponding to the formula $[N6FeOFeCl_3]Cl\cdot 3H_2O\cdot 2CH_3OH\cdot 0.5HCl$, -6.31×10^{-4} cgsu (estimated by using Pascal's constants, including constitutive corrections). Other details of data collection and least-squares analyses have been described elsewhere.[4,5b]

Spectroscopic Studies. Infrared spectra of samples as KBr pellets were recorded on a Perkin-Elmer 457 spectrometer. NMR spectra were recorded on a Bruker 300 using acetonitrile-d_3 as solvent, with a small percent of DMSO d_6 to increase solubility. The Mössbauer spectrum was recorded at Northeastern University; apparatus and techniques have been described elsewhere.[5b] Resonance Raman spectra were recorded at the Oregon Graduate Center, using apparatus and techniques described elsewhere.[5b]

Results and Discussion

Structure of $[N6FeOFeCl_3]^+$. At first glance, the structure of the coordination sphere (Figure 1) resembles very closely that of $[N5FeOFeX_3]^+$ (X = Cl, Br).[5] Three of the four benzimidazole groups and the two amine ligands of N6 encapsulate one iron(III)

(2) Murray, K. S. *Coord. Chem. Rev.* **1974**, *12*, 1–35 and references cited therein.
(3) (a) Sanders-Loehr, J. In *Iron Carriers and Iron Proteins*; Loehr, T. M., Ed.,; VCH: New York, in press. (b) Lippard, S. J. *Angew. Chem. Int. Ed. Engl.* **1988**, *27*, 344–352.
(4) Gomez-Romero, P. Ph.D. Dissertation, Georgetown University, 1987; *Diss. Abs. Int.* **1989**, *50*, 173B, Order No. DA8904779.
(5) (a) Gomez-Romero, P.; DeFotis, G. C.; Jameson, G. B. *J. Am. Chem. Soc.* **1986**, *108*, 851–853. (b) Gomez-Romero, P.; Witten, E. H.; Reiff, W. M.; Backes, G.; Sanders-Loehr, J.; Jameson, G. B. *J. Am. Chem. Soc.* **1989**, *111*, 9030–9047.
(6) Hendriks, H. M. J.; Huinink, W. O. T. B.; Reedijk, J. *Recl. Trav. Chim. Pays-Bas* **1979**, *98*, 499–500. (b) McKee, V.; Zvagulis, M.; Dagdigian, J. V.; Patch, M. G.; Reed, C. A. *J. Am. Chem. Soc.* **1984**, *106*, 4765–4772.

Table II. Positional and Isotropic Displacement Factors for Non-Hydrogen Atoms[a]

atom	x	y	z	B, Å²
Fe1	−0.1507 (1)	0.15991 (7)	0.0509 (1)	3.42 (4)
Fe2	0.0420 (1)	0.22040 (8)	0.1801 (1)	4.04 (4)
Cl1	0.1819 (3)	0.2222 (2)	0.1162 (3)	7.3 (1)
Cl2	0.0708 (3)	0.1962 (2)	0.3343 (3)	7.6 (1)
Cl3	−0.0213 (3)	0.2950 (2)	0.1742 (4)	8.7 (1)
Cl11	0.2727 (8)	0.0938 (4)	0.5083 (7)	8.7 (3)
Cl12	0.0536 (5)	0.5273 (3)	0.377 (1)	20.8 (4)
O1	−0.0357 (6)	0.1784 (3)	0.1138 (6)	4.1 (2)
OW1	0.429 (1)	0.1326 (5)	0.3888 (9)	11.0 (4)
OW2	0.241 (1)	0.8918 (7)	0.362 (1)	20.3 (6)
OW3	0.374 (1)	0.9770 (7)	0.370 (2)	21.4 (7)
O100	0.055 (1)	0.8832 (5)	0.3030 (9)	9.9 (4)
O200	0.285 (1)	0.5353 (5)	0.264 (1)	18.8 (5)
N1	−0.2899 (8)	0.1292 (4)	−0.0435 (8)	4.9 (3)
N2	−0.1607 (7)	0.2107 (4)	−0.0826 (7)	3.7 (3)
N11	−0.0930 (7)	0.1047 (4)	−0.0329 (8)	3.9 (3)
N12	−0.1116 (8)	0.0363 (5)	−0.1278 (9)	5.9 (3)*
N21	−0.2102 (7)	0.1137 (4)	0.1464 (8)	4.2 (3)
N22	−0.3433 (9)	0.0685 (5)	0.188 (1)	6.8 (3)*
N31	−0.2358 (6)	0.2183 (4)	0.0947 (7)	3.5 (2)
N32	−0.2640 (7)	0.3003 (4)	0.0853 (8)	4.5 (3)*
N41	−0.0754 (8)	0.2876 (4)	−0.2304 (8)	4.7 (2)*
N42	−0.0565 (7)	0.2145 (4)	−0.2975 (8)	4.4 (2)*
C1	−0.321 (1)	0.1685 (6)	−0.115 (1)	5.0 (3)*
C2	−0.232 (1)	0.1893 (5)	−0.159 (1)	4.8 (3)*
C11	−0.266 (1)	0.0823 (6)	−0.093 (1)	5.4 (4)*
C12	−0.156 (1)	0.0750 (5)	−0.085 (1)	5.1 (3)*
C13	−0.0147 (9)	0.0419 (5)	−0.099 (1)	4.3 (3)*
C14	0.060 (1)	0.0136 (6)	−0.127 (1)	6.4 (4)*
C15	0.150 (1)	0.0326 (7)	−0.090 (1)	7.5 (4)*
C16	0.168 (1)	0.0722 (6)	−0.029 (1)	5.5 (4)*
C17	0.0855 (9)	0.1006 (5)	−0.008 (1)	4.3 (3)*
C18	0.0011 (9)	0.0839 (5)	−0.0428 (9)	3.4 (3)*
C21	−0.361 (1)	0.1212 (6)	0.029 (1)	6.3 (4)*
C22	−0.299 (1)	0.1010 (6)	0.122 (1)	6.5 (4)*
C23	−0.269 (1)	0.0619 (5)	0.260 (1)	5.2 (3)*
C24	−0.261 (1)	0.0336 (7)	0.341 (1)	8.6 (5)*
C25	−0.171 (2)	0.0335 (9)	0.400 (2)	11.0 (6)*
C26	−0.088 (1)	0.0618 (6)	0.375 (1)	7.4 (4)*
C27	−0.095 (1)	0.0887 (5)	0.288 (1)	5.2 (3)*
C28	−0.1803 (9)	0.0879 (5)	0.234 (1)	4.5 (3)*
C31	−0.196 (1)	0.2608 (5)	−0.053 (1)	5.0 (3)*
C32	−0.2342 (9)	0.2585 (5)	0.041 (1)	4.0 (3)*
C33	−0.2835 (9)	0.2846 (5)	0.174 (1)	4.1 (3)*
C34	−0.310 (1)	0.3130 (6)	0.256 (1)	5.5 (4)*
C35	−0.320 (1)	0.2857 (6)	0.341 (1)	5.6 (4)*
C36	−0.303 (1)	0.2367 (6)	0.344 (1)	6.1 (4)*
C37	−0.276 (1)	0.2098 (5)	0.267 (1)	5.5 (4)*
C38	−0.2649 (9)	0.2347 (5)	0.1849 (9)	3.9 (3)*
C41	−0.0644 (9)	0.2124 (5)	−0.122 (1)	4.1 (3)*
C42	−0.0636 (9)	0.2387 (5)	−0.215 (1)	4.0 (3)*
C43	−0.0622 (9)	0.2495 (5)	−0.371 (1)	4.7 (3)*
C44	−0.059 (1)	0.2438 (6)	−0.475 (1)	5.5 (4)*
C45	−0.073 (1)	0.2873 (6)	−0.529 (1)	6.6 (4)*
C46	−0.088 (1)	0.3330 (6)	−0.494 (1)	6.5 (4)*
C47	−0.088 (1)	0.3392 (6)	−0.390 (1)	5.7 (4)*
C48	−0.0741 (9)	0.2937 (5)	−0.3332 (9)	3.7 (3)*
C100	−0.009 (2)	0.913 (1)	0.353 (2)	17.1 (9)
C200	0.302 (2)	0.5804 (7)	0.257 (2)	12.2 (7)

[a] Starred values indicate atoms were refined isotropically. Anisotropically refined atoms are given in the form of the isotropic equivalent displacement parameter defined as follows: $(4/3)[a^2B(1,1) + b^2B(2,2) + c^2B(3,3) + ab(\cos\gamma)B(1,2) + ac(\cos\beta)B(1,3) + bc(\cos\alpha)B(2,3)]$.

atom, which is linked to the $FeCl_3$ moiety by a bridging oxo group. The metal–ligand separations (Table III) are not significantly different from those seen in $[N5FeOFeCl_3]^+$.[5] Similarly to $[N5FeOFeCl_3]^+$,[5] there is a significant difference (0.046 (10) Å) in the Fe–O separations involving the tetrahedrally and octahedrally coordinated iron atoms. The Fe–O–Fe bond angle (Table IV) is about 4° greater at 153.2 (4)°, leading to an Fe···Fe separation of 3.440 (2) Å. Other differences in angles around the octahedral iron of comparably small magnitude exist. In addition,

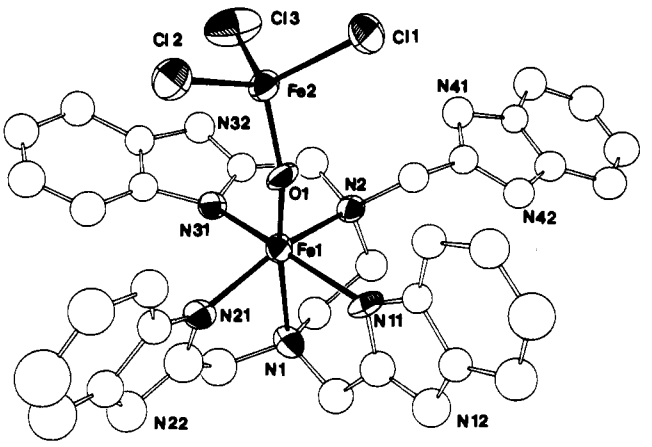

Figure 1. ORTEP diagram of $[N6FeOFeCl_3]^+$. Boundary ellipsoids are drawn at the 40% probability level. Only those atoms refined anisotropically are drawn with shading. For the complete atom labeling, see the diagram of N6.

Table III. Selected Bond Distances (Å)[a]

Fe1–O1	1.791 (7)	Fe1–N31	2.088 (9)
Fe1–N1	2.35 (1)	Fe2–Cl1	2.203 (4)
Fe1–N2	2.283 (9)	Fe2–Cl2	2.213 (4)
Fe1–N11	2.090 (9)	Fe2–Cl3	2.188 (4)
Fe1–N21	2.05 (1)	Fe2–O1	1.745 (7)

[a] Numbers in parentheses are estimated standard deviations in the least significant digits.

Table IV. Selected Bond Angles (deg)

O1–Fe1–N1	172.7 (3)	N2–Fe1–N31	78.2 (3)
O1–Fe1–N2	101.3 (3)	N11–Fe1–N21	97.2 (4)
O1–Fe1–N11	95.4 (3)	N11–Fe1–N31	162.4 (3)
O1–Fe1–N21	104.7 (4)	N21–Fe1–N31	89.7 (4)
O1–Fe1–N31	98.4 (3)	Cl1–Fe2–Cl2	108.4 (2)
N1–Fe1–N2	77.9 (3)	Cl1–Fe2–Cl3	109.1 (2)
N1–Fe1–N11	77.4 (3)	Cl1–Fe2–O1	108.6 (3)
N1–Fe1–N21	77.3 (3)	Cl2–Fe2–Cl3	109.5 (2)
N1–Fe1–N31	88.5 (3)	Cl2–Fe2–O1	110.3 (3)
N2–Fe1–N11	88.6 (3)	Cl3–Fe2–O1	110.9 (3)
N2–Fe1–N21	152.7 (3)	Fe1–O1–Fe2	153.2 (4)

the tetrahedral iron, Fe2, is projected in the same direction with respect to the octahedral N5Fe1 moiety as in $[N5FeOFeX_3]^+$. However, the coordinated chloro ligands adopt a clearly different configuration in the N6 diiron species, corresponding to a formal rotation of the $FeCl_3$ moiety about the Fe2–O bond of ca. 180° (or ~60°) (see Table S-VI, torsion angles). The bond lengths and angles of the $OFeCl_3$ moiety are insignificantly different from those seen in the symmetrical complex $[Cl_3FeOFeCl_3]^{2-}$.[7]

The covalency of the $OFeCl_3$ moiety is indicated by the absence of any intermolecular contacts closer than 3.50 Å. The dangling benzimidazole group appears to be partially protonated, as evidenced by the similar N–C separations. The crystal structure features extensive chains of hydrogen-bonded chloride counterions, water, and methanol moieties linking benzimidazole groups. The packing is also controlled by π–π interactions between the latter, as can be seen in Figure S1 (supplementary material).

Magnetic Susceptibility. The low-temperature portion of the data (7–48 K) were fit to the usual Curie–Weiss expression by assuming a mononuclear high-spin Fe(III) impurity, resulting in $\theta = -1.51$ (7) K and impurity $x = 1.91$ (2)%. The high-temperature data (56–300 K), corrected for the paramagnetic impurity, were fit to the exchange-coupled Hamiltonian, as described elsewhere,[5b]

$$\mathcal{H} = -2JS_1 \cdot S_2$$

giving a value for $-J$ of 126.6 (7) cm^{-1}. The resultant fit is shown

(7) Drew, M. G. B.; McKee, V.; Nelson, S. M. *J. Chem. Soc., Dalton Trans.* **1978**, 80–84.

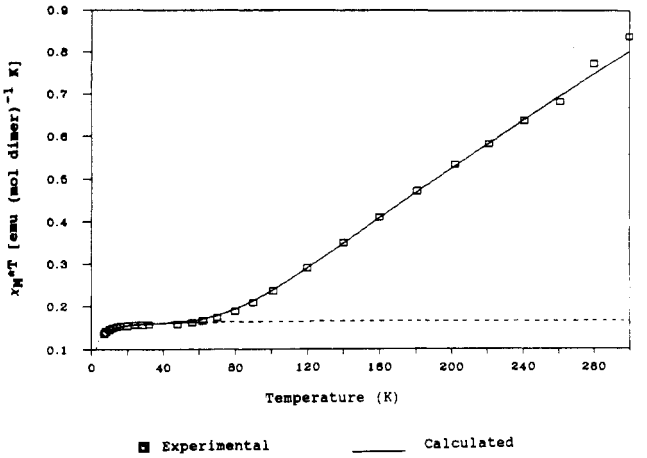

Figure 2. Plot of magnetic susceptibility data as χT vs T for $[N6FeOFeCl_3]^+$. The dotted line shows the contribution from the paramagnetic impurity.

in Figure 2. The diamagnetic correction used corresponds to the composition found in the crystal structure (in good agreement with chemical analyses); the only likely alteration of this composition during the handling of the sample is a partial loss of solvate molecules. Such an event would result in a slightly larger magnitude of the refined coupling constant: thus, the magnitude of the value reported represents a lower bound.

With the exception of porphyrinato species for which $129 < -J < 147$ cm^{-1},[8] the antiferromagnetic coupling constants for other symmetrically coordinated, singly bridged (μ-oxo)diiron(III) species are remarkably independent of the nature of the ligands (N_{amine}, N_{imine}, OH_2, ^-OOCR, Cl^-) and of the coordination number of the iron atoms (4, 5, 6, or 7),[2,7,9] with $92 < -J < -110$ cm^{-1}. Triply bridged species exhibit greater antiferromagnetic coupling, $115 < -J < 121$ cm^{-1} (see also Table IV of ref 5b), presumably due to the weak contribution of the two additional carboxylato bridging ligands.[3,10] Comparison of the asymmetric complexes $[N5FeOFeCl_3]Cl$[5] and $[N6FeOCl_3]Cl$ with other singly bridged non-porphyrinato iron complexes indicates that the values for $-J$ of 122 (1) and 126.6 (6) cm^{-1}, respectively, are anomalously large. Since the crystal structures of $[N5FeOFeCl_3]^+$ and $[N6FeOFeCl_3]^+$ are different, the high values for $-J$ are, therefore, intrinsic to the cation and are not an artifact of secondary coupling by, for example, hydrogen-bonding networks or of other factors, such as impurities. The small difference in values ($\sim$4 (1) cm^{-1}) between the N5 and N6 species is considered at this time to be of marginal significance and not to be ascribed exclusively to the change in bond angle, given that the orientation of the $FeCl_3$ moiety is different in the two complexes.

It has been suggested[9a] that tight binding in the Fe–O–Fe moiety may lead to stronger antiferromagnetic coupling, as may be seen by some of the μ-oxo Fe(III) porphyrinato and phthalocyanato species. While this may be a factor for these systems, there is little support for this hypothesis in non-porphyrinato systems. To wit, for the complex $[Cl_3FeOFeCl_3]^{2-}$ the Fe–O separation of 1.755 Å sits at the low end of the range of Fe–O separations in (μ-oxo)diiron(III) systems while the value for $-J$ lies also at the low end of the range. Moreover, by the tight-binding argument, the value of $-J$ for the unsymmetrical complexes, where the Fe–O separations are 1.751 (4) and 1.782 (4) Å for the N5 complex and 1.745 (7) and 1.797 (7) Å for the N6 complex, should fall in the middle of the range. This is clearly not so.

When two magnetic orbitals from different metal centers can overlap with the same filled orbital of a bridging atom, the two corresponding spins will be antiferromagnetically coupled, whereas if one of the magnetic orbitals overlaps with a bridging ligand orbital to which the other magnetic orbital is orthogonal, this will lead to ferromagnetic coupling of the spins.[11] Symmetrical dinuclear species (L = L') possess to a first approximation C_{2v} symmetry. Therefore, only the interactions depicted in Figure 3a, where like atomic orbitals from both Fe atoms are related by the 2-fold axis, are allowed by symmetry for the antiferromagnetic coupling of electron spins. In this figure, only the interactions through filled 2p (O) orbitals have been considered since these are the closest in energy to the d orbitals of the metals; inclusion of oxygen s-orbital character does not affect the analysis. Furthermore, for clarity, the metal d orbitals are referenced to the C_2 symmetry axis and not to a local molecular axis (e.g. the Fe–O bond, which would complicate but not affect the analysis, especially for a nonlinear Fe–O–Fe moiety). Note also that since the D_{xy} orbital has symmetry a_2 and none of the oxo group's orbitals belongs to this class, no indirect overlap between these metal orbitals is expected.

On the other hand, for unsymmetrical complexes, such as $[N5FeOFeCl_3]^+$ or $[N6FeOFeCl_3]^+$, the idealized symmetry is C_s. As illustrated in Figure 3b, the lower symmetry allows for additional antiferromagnetic interactions among *all* d orbitals from the metals and filled p orbitals from the oxo bridge. In this case, only one symmetry element (Fe–O–Fe mirror plane) imposes constraints on the orbital interactions that lead to antiferromagnetic coupling of electron spins. For example, orbitals d_{xz} (Fe) and d_{yz} (Fe'), which are orthogonal in C_{2v}, are nonorthogonal in unsymmetrical dinuclear species. Low symmetry, which leads to additional magnetic orbitals for antiferromagnetic exchange, provides a necessary but not sufficient condition for stronger antiferromagnetic coupling. For example, a mildly unsymmetrical doubly bridged complex, that has, trans to the oxo bridge, an imine at one iron and an amine at the other, shows antiferromagnetic coupling of $-J = 119$ cm^{-1},[12] close to that expected in the class of triply bridged dinuclear iron(III) systems, and the unsymmetrical complex $[N5FeOFeBr_3]Br$ shows reduced coupling when compared to its chloro analogue. Thus, the differences in ligand fields subtended at the two iron centers are a second factor in determining the strength of the antiferromagnetic coupling. In other words, when the atomic orbitals on each metal center (as perturbed by the local ligand fields) are not dissimilar in energy, stronger antiferromagnetic coupling may be expected in unsymmetrical diiron(III) μ-oxo systems. In addition, the apparently weaker coupling for the complex $[N5FeOFeBr_3]^+$ may be a consequence of the covalent Fe–Br bonds delocalizing spin density

(8) (a) Moss, T. H.; Lillienthal, H. P.; Moleski, C.; Smythe, G. A.; McDaniel, M. C.; Caughey, W. S. *J. Chem. Soc., Chem. Commun.* **1972**, 263–264. (b) Strauss, S. H.; Pawlik, M. J.; Skowyra, J.; Kennedy, J. R.; Anderson, O. P.; Spartalian, K.; Dye, J. L. *Inorg. Chem.* **1987**, *26*, 724–730. (c) Helms, J. H.; ter Haar, L. W.; Hatfield, W. E.; Harris, D. L.; Jayaraj, K.; Toney, G. E.; Gold, A.; Mewborn, T. D.; Pemberton, J. R. *Inorg. Chem.* **1986**, *25*, 2334–2337. (d) A value of $-J = 105$ cm^{-1} is reported for a μ-oxo derivative of a face-to-face bis[(porphyrinato)-iron(III)] system,[8e] where, in addition to a significantly bent Fe–O–Fe moiety (161°), there is a strong hydrogen bond between the μ-oxo and a water. (e) Landrum, J. T.; Grimmett, D.; Haller, K. J.; Scheidt, W. R.; Reed, C. A. *J. Am. Chem. Soc.* **1981**, *103*, 2640–2650.

(9) (a) Ou, C. C.; Wollman, R. G.; Hendrickson, D. N.; Potenza, J. A.; Schugar, H. J. *J. Am. Chem. Soc.* **1978**, *100*, 4717–4724. (b) Plowman, J. E.; Loehr, T. M.; Schauer, C. K.; Anderson, O. P. *Inorg. Chem.* **1984**, *23*, 3553–3559. (c) Mukherjee, R. N.; Stack, T. D. P.; Holm, R. H. *J. Am. Chem. Soc.* **1988**, *110*, 1850–1861. (d) The conclusions that were qualified in ref 9c are stated without equivocation as the "strong antiferromagnetic coupling between the two high-spin Fe(III) that is dependent on FeOFe angle" in: Synder, B. S.; Patterson, G. S.; Abrahamson, A. J.; Holm, R. H. *J. Am. Chem. Soc.* **1989**, *111*, 5214–5223.

(10) Gomez-Romero, P.; Casan-Pastor, N.; Ben-Hussein, A.; Jameson, G. B. *J. Am. Chem. Soc.* **1988**, *110*, 1988–1990.

(11) (a) Anderson, P. W. In *Solid State Physics*; Seitz, F., Turnbull, D., Eds.; Academic Press: New York, 1963; Vol. 14, p 99. (b) Goodenough, J. B. *Magnetism and the Chemical Bond*; Interscience: New York, 1963. (c) Kanamori, J. *Phys. Chem. Solids* **1959**, *10*, 87. (d) Martin, R. L. In *New Pathways in Inorganic Chemistry*; Ebsworth, E. A. V., Maddock, A. G., Sharpe, A. G., Eds.; Cambridge University Press: London, 1968; Chapter 9, pp 175–231.

(12) Yan, S.; Cox, D. D.; Pearce, L. L.; Juarez-Garcia, C.; Que, L., Jr.; Zhang, J. H.; O'Connor, C. J. *Inorg. Chem.* **1989**, *28*, 2509–2511. (b) Actually one might argue that, relative to a single oxo bridge, each carboxylato bridge in triply bridged species contributes $\sim$10 cm^{-1} to $-J$,[3] leading to a prediction of $\sim$110 cm^{-1} for $-J$ in this doubly bridged species.[12a]

Figure 3. Magnetic orbital interactions leading to antiferromagnetic contributions to the coupling of the electron spins of a pair of iron atoms in dinuclear species, under (a) C_{2v} symmetry and (b) C_s symmetry.

away from the Fe–O–Fe moiety.[13] For Fe–Cl bonds in $[FeCl_4][Fe(bpy)_2Cl_2]$ a modest spin delocalization of 0.23 e^-/Cl has been quantified by polarized neutron diffraction.[14]

Recently, an apparent dependency of J on the Fe–O–Fe (and also Fe–S–Fe) bond angle was deduced. In the case of the oxo-bridged complexes of electronically similar but sterically dissimilar Schiff bases, this amounted to an increase in $-J$ of ~8 cm^{-1} for an increase in bond angle of 28°.[9c,d] However, in these systems, not only is there a change in bond angle but also there is a clear change in symmetry. The less antiferromagnetic system is associated not only with the complex with the smaller Fe–O–Fe (Fe–S–Fe) angle but also with the complex that more nearly approximates C_{2v} symmetry. A possible angle dependency was claimed for a pair of (μ-oxo)bis[(phthalocyanto)iron(III)] complexes, where a value of $-J$ = 120 cm^{-1} was associated with a bent Fe–O–Fe moiety and a value of $-J$ = 195 cm^{-1} with a linear Fe–O–Fe moiety; however, neither species has been definitively characterized by single-crystal diffraction methods.[15] Further, as noted above for the complexes $[N6FeOFeCl_3]Cl$ and $[N5FeOFeCl_3]Cl$, although the larger value of $-J$ is associated with the complex with the larger Fe–O–Fe bond angle, the difference in J is not statistically significant and the bond angle is not the only conformational parameter to change. Thus, evidence for a dependence of J on the Fe–O–Fe bond angle remains equivocal.

For oxyhemerythrin the apparently weaker antiferromagnetic coupling (J = −77 cm^{-1})[16] may be attributed to the hydrogen bonding of the hydroperoxo moiety to the oxo bridge, which has been observed by resonance Raman spectroscopy,[17] between the coordinated hydroperoxo moiety $-OOH^-$ and the μ-oxo bridge, giving partial hydroxo character to the latter. A (μ-oxo)bis[(porphyrinato)iron(III)] species with the μ-oxo moiety hydrogen-bonded to a water molecule also shows reduced antiferromagnetic coupling[8d,e] relative to other porphyrinato species.[8a-c] However, from recent NMR experiments a less pronounced difference in antiferromagnetic coupling between oxyhemerythrin and methemerythrin was inferred.[18] The determination of magnetic behavior based upon chemical shifts of protons of the molecule, rather than of an external reference, is rather approximate and susceptible to geometric factors and changes in geometry with temperature, which affect the amount of spin density transferred from the metal center onto its ligands.[19] The large magnitude of the observed coupling for methemerythrin (J = −134 cm^{-1}) is reasonable, since the dinuclear iron cluster has both a triply bridged configuration and an asymmetric distribution of ligands. The even greater coupling for purple acid phosphatase

(13) Noodleman, L. Personal communication.
(14) Figgis, B. N.; Reynolds, P. A.; Forsyth, J. B. *J. Chem. Soc., Dalton Trans.* **1988**, 117–122.
(15) (a) Ercolani, C.; Gardini, M.; Murray, K. S.; Pennesi, G.; Rossi, G. *Inorg. Chem.* **1986**, *25*, 3972–3976. (b) Kennedy, B. J.; Murray, K. S.; Zwack, P. R.; Homborg, H.; Kalz, W. *Inorg. Chem.* **1985**, *24*, 3302–3305.
(16) Dawson, J. W.; Gray, H. B.; Hoenig, E.; Rossman, G. R.; Schredder, J. M.; Wang, R.-H. *Biochemistry* **1972**, *11*, 461–465.
(17) Shiemke, A. K.; Loehr, T. M.; Sanders-Loehr, J. *J. Am. Chem. Soc.* **1986**, *108*, 2437–2443.
(18) Maroney, M. J.; Kurtz, D. M., Jr.; Nocek, J. M.; Pearce, L. L.; Que, L., Jr. *J. Am. Chem. Soc.* **1986**, *108*, 6871–6879.
(19) Morris, N. L. Ph.D. Dissertation, Georgetown University, 1989.

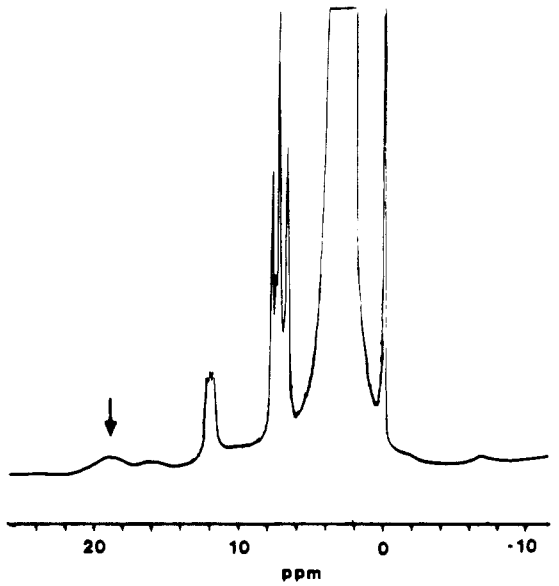

Figure 4. ^1H NMR spectrum of $[N6FeOFeCl_3]^+$ in acetonitrile d_3 (+DMSO-d_6), showing the resonance (arrowed) attributed to the exchangeable N–*H* protons.

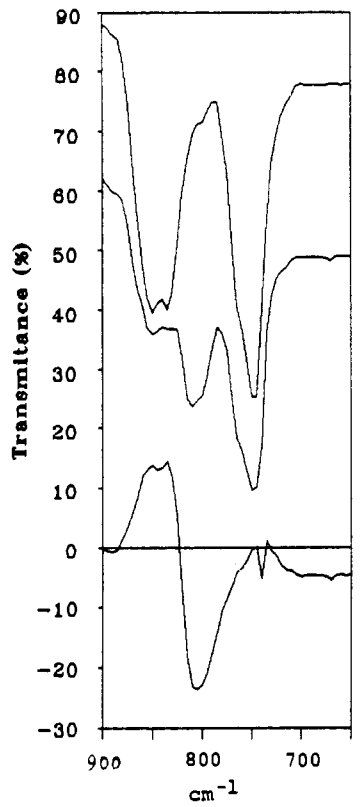

Figure 5. Infrared spectra for $[N6FeOFeCl_3]Cl$ in the region of ν_{as}(Fe–O–Fe): (top) ^{16}O derivative; (middle) ^{18}O derivative; (bottom) difference.

($J < -150$ cm^{-1})[20] is consistent with the known asymmetry of iron ligands in that protein—in particular the anionic phenolate ligands congregated around only one iron atom.[17]

^1H NMR Spectroscopy. In acetonitrile solution the N–*H* resonances are seen by means of D_2O exchange at 19 ppm for the coordinated benzimidazole groups. The protons on the uncoordinated partially protonated benzimidazole could not be detected (Figure 4). This value is similar to those seen in the

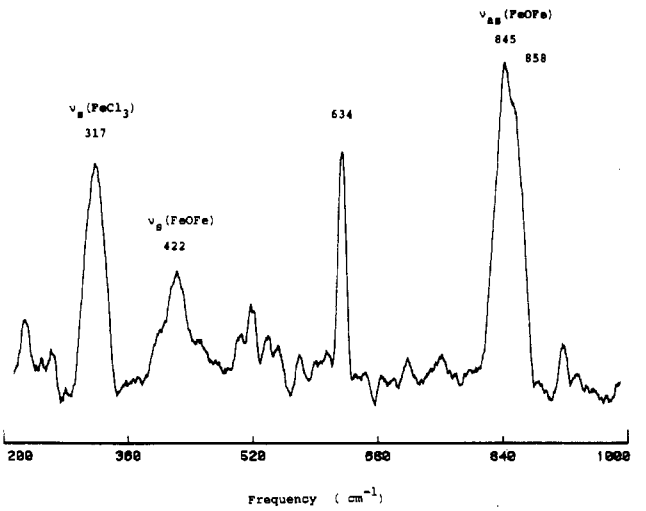

Figure 6. Resonance Raman spectrum for $[N6FeOFeCl_3]Cl$.

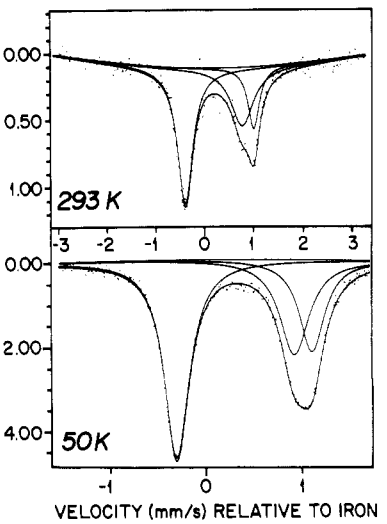

Figure 7. Mössbauer spectra of $[N6FeOFeCl_3]^+$ at 50 and 293 K.

oxo-bridged diiron(III) systems[5,10] and methemerythrin.[3]

Vibrational Spectroscopy. As with the N5 analogues, a strong doublet, in this instance at 833 and 850 cm^{-1}, collapses to a broad unsymmetrical peak at 800 cm^{-1} upon substitution of the bridging oxo group by ^{18}O (Figure 5). In the resonance Raman spectrum ν_{as}(Fe–O–Fe) is seen at 845 cm^{-1} and ν_s(Fe–O–Fe) at 422 cm^{-1} by analogy with the ^{16}O and ^{18}O derivatives of $[N5FeOCl_3]^+$. Again, atypically for symmetrical and mildly unsymmetrical (μ-oxo)diiron(III) species, including methemerythrin derivatives, the ratio of intensities of the asymmetric and symmetric Fe–O–Fe stretches is anomalous for the present case, with $I_{as}/I_s > 1$.[4,5b,21] The symmetric Fe–Cl_3 stretch is seen at 317 cm^{-1}. The other significantly enhanced mode at 634 cm^{-1} that is common to $[NmFeOFeX_3)^+$ species (m = 5, 6; X = Br, Cl) remains unassigned. The resonance Raman spectrum is illustrated in Figure 6. A precise understanding of this reversal of enhancement for unsymmetrical species in terms of the nature of the changes in the polarizability tensor is not available yet. However, in the complexes with identical or similar ligands and ligand numbers at each iron center, the dipole moment vector is aligned at least approximately perpendicular to the Fe··Fe vector and in the plane of the Fe–O–Fe fragment. On the other hand, in complexes with dissimilar ligands and ligand numbers, the dipole moment vector is canted toward the Fe··Fe vector.

Mössbauer Spectroscopy. Two pairs of quadrupole doublets are seen at both 293 and 50 K; one peak of each doublet is

(20) Averill, B. A.; Davis, J. C.; Burman, S.; Zirino, T.; Sanders-Loehr, T. M.; Sage, J. T.; Debrunner, P. G. *J. Am. Chem. Soc.* **1987**, *109*, 3760–3767.

(21) Sanders-Loehr, J.; Wheeler, W. D.; Shiemke, A. K.; Averill, B. A.; Loehr, T. M. *J. Am. Chem. Soc.* **1989**, *111*, 8084–8093.

completely overlapped, as shown in Figure 7. The parameters for the tetrahedral iron [δ = 0.18 and ΔE_q = 1.16 mm s^{-1} (293 K); δ = 0.30 and ΔE_q = 1.22 mm s^{-1} (50 K)] are assigned by comparison with the symmetrical $[Cl_3FeOFeCl_3]^{2-}$ complex.[7] For the octahedral iron the isomer shift [δ = 0.29 (293 K) and 0.40 mm s^{-1} (50 K)] is at the bottom end of the range observed for symmetrical bisoctahedral (μ-oxo)diiron(III) systems.[22] This low value is attributed to perturbation from the $OFeCl_3$ moiety. Similar behavior was observed for the N5 analogues.[5b] The large values for the quadrupole splitting [ΔE_q = 1.40 (293 K) and 1.41 mm s^{-1} (50 K)] are typical of other (μ-oxo)diiron(III) systems and are not significantly different from that for $[N5FeOFeCl_3]Cl$, at least at 293 K—at low temperatures (50 and 77 K, respectively) the Mössbauer spectra are visibly different, with $[N5FeOFeCl_3]Cl$ having perfectly overlapped quadrupole doublets at 77 K.[5b]

Conclusions

In the unsymmetrical complexes, $[NmFeOFeCl_3]^+$, where N*m* provides five nitrogenous ligands to the iron center, the lowered symmetry, C_s, combined with the comparable ligand orbital energies around the dissimilarly coordinated iron centers leads to stronger antiferromagnetic coupling ($-J > 120$ cm^{-1}) than is seen in symmetrical singly bridged species with higher symmetry, C_{2v}. Also characteristic of these unsymmetrical molecular structures is the observation in the infrared spectrum of a strong doublet at ca. 850, 835 cm^{-1} associated with the Fe–O–Fe′ group and in the resonance Raman spectrum of a value greater than unity for the ratio of the intensities of the asymmetric to the symmetric Fe–O–Fe stretch.

Acknowledgment. We gratefully acknowledge the support of the National Institute of Diabetic, Kidney, and Digestive Diseases of the National Institutes of Health through Grant 5 R01 DK37702 (G.B.J.), the Solid State Chemistry Program of the National Science Foundation through Grant DMR 8313710 (W.M.R.), and the Comite Conjunto Hispano-Norteamericano para la Cooperacion Cultural y Educativa for a fellowship to P.G.-R. We thank Dr. Joann Sanders-Loehr and Jinshu Ling for the resonance Raman spectrum, Dr. Ekk Sinn and Dr. Thitinant Thanyasiri for the collection of magnetic susceptibility data, and Dr. Nieves Casaon-Pastor and Dr. Nancy Morris for recording the NMR spectra.

Registry No. N_6·HCl, 129240-50-2; $[N_6FeOFeCl_3]Cl·3H_2O·2CH_3OH·0.5HCl$, 129264-58-0.

Supplementary Material Available: Tables of full crystal and refinement data (Table S-I), atomic and isotropic thermal parameters (Table S-II), anisotropic displacement parameters (Table S-III), bond distances (Table S-IV), bond angles (Table S-V), torsion angles (Table S-VI), and rms amplitudes of anisotropic displacement (Table S-VII) and a unit cell diagram (Figure S-1) (12 pages); a listing of structure factors (43 pages). Ordering information is given on any current masthead page.

(22) Gibb, T. C.; Greenwood, N. N. In *Mössbauer Spectroscopy*; Chapman and Hall: London, 1971.

Contribution from the Institute of Inorganic Synthesis, Yamanashi University, Miyamae-cho 7, Kofu, 400 Japan

Preparation of an Acid Niobium Phosphate and Alkali-Metal Niobium Phosphates, Having $NbOPO_4·H_2O$ Layers Condensed with the Phosphate Group

Nobukazu Kinomura* and Nobuhiro Kumada

Received May 1, 1990

New alkali-metal niobium phosphates and an acid niobium phosphate were prepared under low temperature hydrothermal conditions. Their chemical formulas were deduced to be $NaNb_2(OH)_2(PO_4)_3·2.5H_2O$, $KNb_2(OH)_2(PO_4)_3·nH_2O$, and $HNb_2(OH)_2(PO_4)_3·H_2O$, having lattice constants of a = 6.488 (2) Å and c = 16.286 (5) Å in the tetragonal system, a = 6.489 (3) Å, b = 6.452 (2) Å, c = 16.149 (6) Å, and β = 95.63 (3)° in the monoclinic system, and a = 6.485 (2) Å, b = 6.415 (3) Å, c = 16.18 (2) Å, α = 90.11 (7)°, β = 95.91 (5)°, and γ = 90.95 (5)° in the triclinic system, respectively. They are isostructural, having a three-dimensional structural framework composed of $NbO(H_2O)(PO_4)$ layers combined with PO_4 groups. The alkali-metal ions and protons are exchangeable with other alkali-metal, alkaline-earth-metal, and alkylammonium ions. The acid niobium phosphate can intercalate *n*-alkylamines. The PO_4 group that links the layers is removed upon ion exchange with certain ions and upon intercalation with certain amines, and the three-dimensional structure is transformed to a layered structure.

Introduction

Vanadium phosphate shows a reversible change from an anhydrous three-dimensional structure for α-$VOPO_4$ to hydrated layered structures for $VOPO_4·nH_2O$.[1] The crystal structure of $VOPO_4·2H_2O$, which was analyzed by Teitze,[2] consists of layers of $VO_5(H_2O)$ octahedra and PO_4 tetrahedra that share corners and water molecules in the interlayer spaces connecting the layers. In the system Nb_2O_5–P_2O_5–H_2O, similar anhydrous and hydrated niobium phosphates were reported,[3-5] but the change from hydrated phase to dehydrated phase was irreversible.

Beneke and Lagaly[6] reported that $NbOPO_4·nH_2O$ can intercalate various types of amines in the interlayer spaces. Niobium phosphates that contain neutral acid molecules H_3PO_4 and H_2SO_4 and water molecules in the interlayer spaces were also prepared, but the acid was removed with ease by washing with water.[6,7] Beneke and Lagaly[6] also mentioned preparation of the layered acid niobium phosphate $Nb_2(OH)_2(HPO_4)(PO_4)_2·4.4H_2O$, which is composed of two layers of $Nb(OH)_2PO_4$ connected by the PO_4 group, as if the neutral H_3PO_4 intercalated into the interlayer spaces condensed to link the layers.

We report here the preparation of alkali-metal niobium phosphates and an acid niobium phosphate with three-dimensional structures and their ion-exchange and intercalation behaviors.

Experimental Section

Preparation. Two kinds of starting material were used in this study: amorphous niobium oxide and sodium polyniobate, $Na_8Nb_6O_{19}·13H_2O$. The preparative method for $Na_8Nb_6O_{19}·13H_2O$ was described elsewhere.[8] The amorphous starting material was prepared by fusing niobium pentaoxide with K_2CO_3, dissolving in water, and precipitating with hydro-

(1) Ladwig, G. *Z. Anorg. Allg. Chem.* **1965**, *338*, 266.
(2) Tietze, H. R. *Aust. J. Chem.* **1981**, *34*, 2035.
(3) Longo, J. M.; Kierkegaad, P. *Acta Chem. Scand.* **1966**, *20*, 72.
(4) Levin, E. M.; Roth, R. *J. Solid State Chem.* **1970**, *2*, 250.
(5) Deulin, G. I.; Dushin, R. B.; Krylov, V. N. *Russ. J. Inorg. Chem.* (*Engl. Transl.*) **1979**, *24*, 1291.
(6) Beneke, K.; Lagaly, G. *Inorg. Chem.* **1983**, *22*, 1503.
(7) Chernorukov, N. G.; Egorov, N. P.; Kutsepin, V. F. *Russ. J. Inorg. Chem* (*Engl. Transl.*) **1979**, *24*, 987.
(8) Kinomura, N.; Kumada, N.; Muto, F. *Mater. Res. Bull.* **1984**, *19*, 299.

0020-1669/90/1329-5217$02.50/0